

# RSC Advances

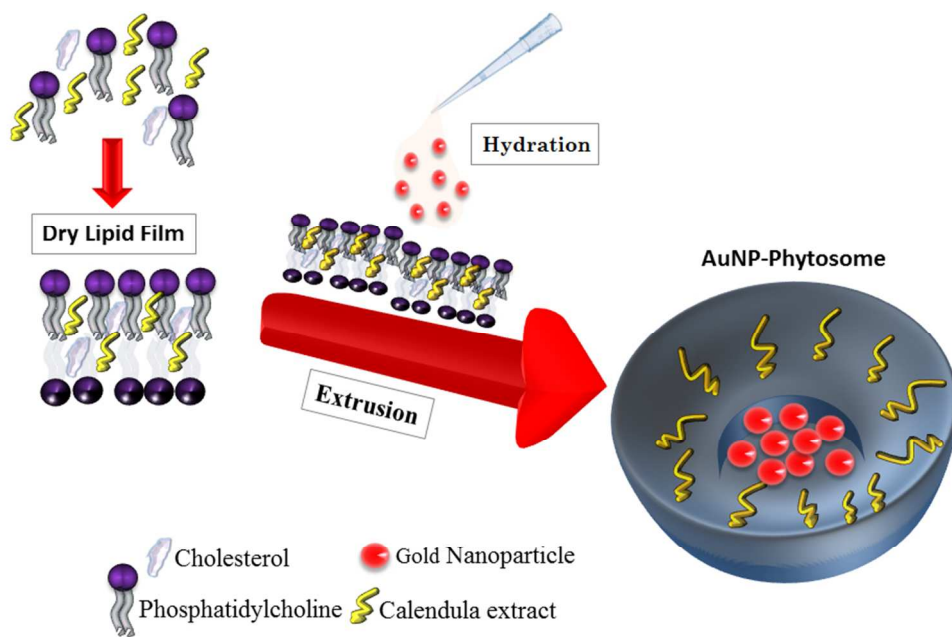


This is an *Accepted Manuscript*, which has been through the Royal Society of Chemistry peer review process and has been accepted for publication.

*Accepted Manuscripts* are published online shortly after acceptance, before technical editing, formatting and proof reading. Using this free service, authors can make their results available to the community, in citable form, before we publish the edited article. This *Accepted Manuscript* will be replaced by the edited, formatted and paginated article as soon as this is available.

You can find more information about *Accepted Manuscripts* in the [Information for Authors](#).

Please note that technical editing may introduce minor changes to the text and/or graphics, which may alter content. The journal's standard [Terms & Conditions](#) and the [Ethical guidelines](#) still apply. In no event shall the Royal Society of Chemistry be held responsible for any errors or omissions in this *Accepted Manuscript* or any consequences arising from the use of any information it contains.



254x190mm (96 x 96 DPI)

## ARTICLE

# Gold Nanoparticle Loaded Phytosomal Systems: Synthesis, Characterization and *in vitro* Investigations

Cite this: DOI: 10.1039/x0xx00000x

Received 00th January 2012,  
Accepted 00th January 2012

DOI: 10.1039/x0xx00000x

www.rsc.org/

B. Demir,<sup>a</sup> F. B. Barlas,<sup>a</sup> E. Guler,<sup>a</sup> P. Z. Gumus,<sup>b</sup> M. Can,<sup>c</sup> M. Yavuz,<sup>a,d</sup> H. Coskunol,<sup>b,e,f</sup> S. Timur,<sup>a,b\*</sup>

Most of the medicinal and pharmaceutical herbal extracts are poorly soluble in aqueous moieties and have reduced adsorption by living cells. Liposomal encapsulation of those so called phytosomes could be a solution to overcome this problem. Meanwhile, many research showed that metallic nanoparticles such as gold nanoparticles (AuNPs) exhibited biological activity such as wound healing and antioxidant upon living cells. Here, we constructed a novel liposomal formulation by encapsulating both *Calendula officinalis* extract and AuNPs. After the preparation of vesicles using the traditional thin film hydration method within extrusion, resulted AuNP-phytosomes were characterized by dynamic light scattering size measurements, zeta potential and atomic force microscopy respectively. These vesicles are under the size of 100 nm and have a high encapsulation efficiency of chlorogenic acid and quercetin as the model major molecules of *Calendula* extract. Furthermore, AuNP-phytosomes exhibited antioxidant and wound healing activity significantly according to free forms of each encapsulated materials and plain liposome as well as phytosome form. Moreover, the cellular interactions of the vesicles were monitored using the nano-vesicles prepared by Texas-Red labelled lipids under fluorescence microscopy.

## 1. Introduction

Liposomes are spherical vesicles formed from polar lipids and having an aqueous core with an enclosed structure of phospholipid bilayer membrane. For the past two decades liposomes have become a hot topic thanks to their excellent properties, creating effective platforms for enhancing bioavailability of hydrophobic materials to utilize in drug delivery of oral and topical formulations, contrast imaging agents, protein delivery and gene therapy.<sup>1</sup>

Many polyphenolic and flavonoid compounds which have used to be derived from plants are known for the cornerstone of the medicinal nutrients such as phytomedicines and applied in health maintenance and disease management since the dawn the beginning of history. Most of these phytomedicinal compounds, especially phenolics, are poorly-adsorbed in the body by posing a challenge in clinical applications.<sup>2</sup> In order to solve this problem, many strategies have been developed to enhance the bioavailability of phytomedicines from plant extracts such as encapsulation in liposomes, micelles and polymeric particles.<sup>3</sup> Phospholipids as the major compound of liposomal membrane can generate complexes with natural active ingredients and constitutes "Phytosomes" which was emerged as a new technology in 1989.<sup>4</sup> Phytosomes are obtained by chemically reacted with selected herbal extracts and phospholipid preparation (mainly derived from hydrogen bonds), consisting mainly of phosphatidylcholine (PC), which is also the major phospholipid of

living tissues. The produced phytosome complex is investigated for bioavailability and biological efficiency, usually compared to its non-phytosome form.<sup>5</sup> Some of the advantages of phytosomes are as followed; 1) increasing the absorption rate of lipid insoluble polar phytomaterials resulting greater therapeutic benefit, 2) decrease of the required dose, 3) within the formation of chemical bonds, more stable formulations can be achieved.<sup>6</sup> In this regard, Hou et al., prepared a formulation system based on phytosomes loaded with mitomycin C – soybean phosphatidylcholine complex by solvent evaporation combined with a nanoprecipitation technique in order to evaluate its anti-tumor effect.<sup>7</sup> In the other reported studies are also showed the enhanced bioactivity of phytosomal complexes such as hepatoprotective, anti-inflammatory, antioxidant and anticancer activity by generating daidzein, salvianolic acid B, clarithromycin, rutin, 10-hydroxycamptothecin, oxymatrine, luteolin, curcumin, silybin and valproic acid phospholipid complexes.<sup>8</sup>

*Calendula officinalis* Linn which belongs to Astraceae (Compositae) family and named as "Calendula or marigold" has been widely used for ornamental and medicinal purposes as folk therapy.<sup>9</sup> Owing to its pharmacological activity, *Calendula* has been utilized at anti-tumoral<sup>10</sup>, anti-inflammatory, wound healing<sup>11</sup> and antioxidant activities<sup>12</sup> and in 200 cosmetic products in its extracted form<sup>13</sup>. In the prevention of acute dermatitis in cancer patients, *Calendula* was highly efficacious at undergoing postoperative irradiations.<sup>14</sup>

Gold nanoparticles (AuNPs) have attracted among most researchers related to their unique size- and shape-dependent properties based on the surface plasmon resonance. AuNPs are known as inert and relatively less cytotoxic nanomaterials. Due to their reduced toxicity, AuNPs could be used in drug delivery, gene delivery and imaging agents as bioconjugated structures. Many reviews indicate the AuNPs and their biomedical applications, recently.<sup>15</sup> On the past decade, AuNPs were observed in vesicular systems such as polymeric nanoparticles and liposomes as well.<sup>16</sup> Complexes of liposomes and AuNPs have gained attention in the applications of therapeutic and theranostic structures.<sup>17</sup> Moreover, it is shown that liposomes can be stabilized by the addition of AuNPs by Michel et al.<sup>18</sup>

Herein, we established a novel vesicular formulation by encapsulation of AuNPs and Calendula extract into the liposomes (so called phytosomes). As mentioned above, there are many studies about both herbal nutrients containing phytosomes and AuNPs-liposome complexes. However, as our best knowledge, there is no reported study on the incorporation of Calendula and AuNPs into spherical lipid membranes and their evaluation in terms of biological activities as well as some of physicochemical properties. After the synthesis of AuNP-phytosomes, particle size, zeta potential and short term stability tests were accomplished. Then, biological activities such as cytotoxicity, antioxidant capacity and wound healing of resulting formulations were examined. Finally, to investigate the cell penetration of AuNP-phytosomes, cell imaging studies was carried out via fluorescence microscopy. Plain liposomes and phytosomes without AuNPs were tested during all the experiments as the control.

## 2. Material and Method

**Chemicals and reagents.** Egg Phosphatidylcholine (99 %) (PC) and cholesterol (ovine wool 98%) (Chol) were purchased from Avanti (Avanti Polar Lipids Inc. Alabaster, Alabama, USA). Gold nanoparticles (10 nm) were obtained from BBI Solutions (Cardiff, UK). Cell Culture media minimal Essential Medium (MEM), fetal bovine serum (FBS), L-glutamine, penicilin, streptomycin, 3-(4,5-dimethylthiazol-2-yl)-2,5-diphenyl tetrazoliumbromide (MTT), sodium dodecyl sulphate, chlorogenic acid, quercetin, diamino-2-phenylindol (DAPI), was purchased from Sigma Aldrich (Dorset, UK). Texas-Red® 1,2-Dihexadecanoyl-sn-Glycero-3-Phosphoethanolamine Triethylammonium Salt (Texas-Red-DHPE) was obtained from InvitroGen (Eugene, OR.). All other solvents like methanol and chloroform were purchased from Sigma Aldrich (Dorset, UK).

**C. officinalis extract.** Initially, *C. officinalis* were dried and powdered. Then, powdered flowers were extracted at room temperature in methanol for 6 h via solvent extraction method.<sup>19</sup> The extract was then filtered. The filtrate was freeze-dried and kept under vacuum to obtain a concentrated crude extract.

**Liposomes.** Liposomes were prepared using conventional thin film hydration method. PC and Chol 3:1 as a mg ratio in all experiments. A lipid mixture was prepared dissolving them with chloroform in a 50 mL round bottom flask. Evaporation of chloroform was carried out with a Buchi-RII Rotavapor model evaporator (BÜCHI Labortechnik AG, Flawil, Switzerland) equipped with a vacuum pump. Thin film was hydrated with phosphate buffer saline (PBS, pH 7.4) and incubated overnight above T<sub>m</sub> temperature of lipids. Later, vigorous vortexing was applied during 10 min to form lipid vesicles. In order to get a

narrow sized vesicle distribution, liposome suspension was passed through in an extruder (Avanti Polar Lipids Inc. Alabaster, Alabama, USA) 10 times using a 80 nm polycarbonate membrane. As a final step, extruded liposomes were dialyzed against distilled water overnight. Prepared samples were stored at +4 °C protecting from light for further use.

**AuNP loaded phytosomes.** The same procedure was used during the preparation of *C. officinalis* and AuNP loaded liposomes. Briefly, Calendula extract was added with PC and Chol prior to generating thin film layer as the mg ratio of 3:1:1 (PC:Chol:Calendula). Since the hydration process occurred, AuNP (10 nm) was added at the ratio of 1:19 to Phosphate buffer saline (PBS, 50 mM, pH 7.4). After the incubation over T<sub>m</sub> temperature of lipids, vesicles were extruded 10 times and dialyzed overnight. Phytosomes were kept in the same conditions as liposomes.

**Characterization.** Size distribution and zeta potential of liposomes were measured by a dynamic light scattering (DLS) method with Zetasizer Nano ZS (Malvern Instruments Ltd., U.K.) at a scattering angle of 90° using a wavelength of 633 nm and at 25 °C. Prior to measurements, the samples (50 µL) were diluted to 1.0 mL with PBS and each sample was measured three times. Zeta potential of samples was calculated by the device according to Smoluchowski equation. Furthermore, size and zeta potential dependent stability was carried out using DLS method thorough 20 days. All samples were kept in +4 °C during the stability assays.

AFM measurements were carried out at ambient conditions by using an NT-MDT NTEGRA SOLARIS. The non-contact mode (tapping mode) was used for topographic images. A 10 µm scanner equipped with silicon tips with 10 nm tip curvature and an ITO coated glass substrate was used for measurements. To clean the surface of indium tin oxide (ITO), ITO coated glasses were sonicated successively for 15 min, in detergent solution, and then washed with deionized water, acetone and 2-propanol, respectively. After drying in N<sub>2</sub> stream, 1.0 mg mL<sup>-1</sup> solution of liposomes were immediately spin coated on the ITO substrates at 20 °C and then directly measured via AFM instruments.

**Encapsulation efficiency (EE).** To eliminate the un-encapsulated Calendula extract, freshly prepared phytosomes were dialyzed for 24 h against to distilled water. Encapsulation efficiency (EE) of phytosomes was determined using the amount of the major components of Calendula extract encapsulated into the vesicular systems. Chlorogenic acid and quercetin as major phenolic and flavonoid, were chosen as the model component to estimate the EE. The dialyzed phytosomes were disrupted with methanol to obtain free components from bilayer membrane structures. Analyses of these compounds were performed via ultra-performance liquid chromatography (UPLC). A Waters Acquity UPLC® H-Class system with a quaternary solvent manager, an automatic sample manager (FTN) device and TUV detector (Waters Corporation, Milford, MA) were used for liquid chromatography analysis. Chromatography column sample solutions were determined by Waters Acquity BEH C18 column (50 mm x 2.1 mm, 1.7 µm). The mobile phase consisted of (A) phosphate buffer (pH 3.0) (B) acetonitrile (75:25, v:v). The flow rate was adjusted to 0.3 mL min<sup>-1</sup>, and the automatic sample feeding room was at 30 °C and 20 °C, respectively. Detection and quantification was carried out at 330 nm for chlorogenic acid and at 200 nm for

quercetin. The analysis of EE is calculated according to the following equation:

$$EE (\%) = \left[ \frac{\text{CA or Quercetin in phytosomes}}{\text{Total CA or Quercetin added}} \right] \times 100$$

#### Cell culture

Vero cell line (Monkey kidney fibroblast like) was used as a model to investigate the biological activities of the liposomes and phytosomes at the cellular level obtained from ATCC. Moreover, *in vitro* wound healing studies were accomplished with Normal Dermal Human Fibroblast (NHDF) cells (Lonza, Basel, Switzerland). The cells (both cell lines) were cultivated in MEM (Minimum Essential Medium Eagle) medium containing fetal calf serum (10%) and penicillin/streptomycin (1.0%) and were incubated in a humidified CO<sub>2</sub> incubator at 37 °C with 5.0% CO<sub>2</sub>.

**Cytotoxicity assay.** The dose-dependent cytotoxicity of the samples was investigated via 3-(4,5 Dimethylthiazol-2-yl)-2,5-diphenyl tetrazolium bromide (MTT) assay.<sup>20</sup> Cells were transferred from flask to 96-well-tissue plates. Cultivation of the cells in the wells was continued until reaching the confluence. The medium was removed and the cells were washed with PBS. After the cells were treated with the vesicular samples (liposomes, phytosomes and Au-phytosomes) at varying concentrations for 2 h, the samples were removed by washing with PBS. After adding 10% MTT solution to the wells (110 µL per well) and incubation of 4 h with MTT reagent, to dissolve formazan which was produced inside the cells as a result of MTT treatment, 100 µL SDS (1.0 g SDS in 10 mL 0.01 M HCl) was added to each well. At the end of 24 h incubation, the optical densities of each well were analyzed with a spectrophotometric plate reader (Bio-Tek Instruments, Inc., Winooski, VT, USA) at 570 nm and 630 nm. In addition, Vero cells were also treated with Calendula extract and AuNPs in PBS as the control.

**Cell-based antioxidant activity.** There are various methods to observe an antioxidant effect via cell culture. In this part, we used a method based on the measurement of the cell viability after H<sub>2</sub>O<sub>2</sub> induced cell death.<sup>21</sup> Vero cells, as model cell line, were grown in 96-well plates until a confluence of 80% is reached. The cells were treated with the samples for 2 h. After pre-treatment, the cells were exposed to H<sub>2</sub>O<sub>2</sub> (1.25 mM) to stimulate oxidative stress. Then, H<sub>2</sub>O<sub>2</sub> treated cells were incubated for 24 h under ideal conditions (5.0% CO<sub>2</sub>, humidified air and 37 °C). Afterwards, the cell viability was determined for the sample treated cells and the cells without any treatment (control) using MTT test (described in cytotoxicity assay part). Cell based antioxidant activity of the samples was described according to the cell viability of the control.

**In vitro Scratch assay for wound healing.** Normal human dermal fibroblast (NHDF) cells were seeded into 24-well plates and mechanical scratch wound were created in the confluent cell monolayer using a sterile pipette tip.<sup>22</sup> Cells were subjected to incubate with the samples (using the same nontoxic dose) and also without any sample as a control, for 1 h, 4 h and 8 h. An inverted microscope (Olympus CKX41) equipped with a CCD camera (Olympus XC30) was utilized for the cell images (with 4x magnification). Wound healing (%) was determined according to cell migration into the scratch wounded area by using a computer program (Image J). For this purpose, the injured area after 4 and 8 h were estimated by reference to gap at 1 h.

**Cell imaging via fluorescence microscopy.** In order to observe the interactions of the prepared vesicles with the Vero cells, the plain liposomes, phytosomes and AuNP-phytosomes were labeled with Texas-Red dye. Labelled lipid films were prepared as the mg ratio of 3:1:1:0.05 (PC:Chol:Calendula:Texas-Red DHPE) for phytosomes and 3:1:0.05 (PC:Chol:Texas-Red DHPE) prior to extrusion step. The cell images were taken via Fluorescence microscope (Olympus BX53F) equipped with a CCD camera (Olympus DP72). To obtain the cell images, the samples (2.0 mg mL<sup>-1</sup> as the total lipid amount) were diluted with medium 1:1 and were added to cells grown in a chamber slide for two days. After treatment for 2 h at 37 °C, the cells were washed twice with PBS. Then, the cells were stained with DAPI. Cell photographs were given as overlapped images of the cells visualized with Texas-Red labelled vesicles and DAPI.

**Statistical analysis.** All experiments were repeated at least three times. All data were expressed as average ± SD (standard deviation) unless particularly outlined. A one-way analysis of variance (ANOVA) was performed with Tukey's multiple comparison test in statistical evaluation. The difference between two groups was considered to be significant when the 'P' value was less than 0.05 and highly significant when the 'P' value was less than 0.01 or 0.001.

## 3. Results and Discussion

### 3.1 Characterization

The fate of nanoparticles is mainly affected by their particle size and size distribution. In addition homogenous size distribution is the fundamental phenomena in order to achieve the excellent physical stability. Zeta potential is a function of the surface charge of the suspension or dispersion, knowledge of which of the liposomal structures can help to predict and control the fate of these vesicles in cell media.<sup>23</sup> After the preparation step of liposomes (PC:Chol), phytosomes (PC:Chol:Calendula) and AuNP loaded phytosomes, dynamic light scattering and zeta potential measurements were performed. As shown in Table 1. The hydrodynamic size of plain liposomes, phytosomes and AuNP loaded phytosomes are 93±6.0, 73±6.0 and 80±5.0 nm, respectively. Besides, the size and zeta potential of the commercial AuNPs were estimated as 8.0±2.0 nm with a -42±7.0 mV surface charge. The particle size of the all vesicle suspensions is close to each other because of using the extrusion process during the vesicle formation.<sup>24</sup> Moreover, their polydispersity index (PDI) is lower than other liposomal preparations.<sup>7, 25</sup> Zeta potential of vesicles decreased when Calendula extract was added to the plain liposome formulation. It is known that cholesterol have an impact on the orientation of polar head group of phospholipids.<sup>26</sup> Negative groups on the polar site head towards to outside of bilayer membrane. Therefore, even neutral lipids like PC can show negative zeta potential. However, it can be clearly seen that, there is a difference between plain liposomes and phytosomes. Hydrophobic compounds of MeOH extract of Calendula may exhibit interference among PC and Chol structures like the other studies based on plant extract based liposomes.<sup>3e, 4</sup> On the other hand, AuNPs in the vesicles did not show a significant alteration in the surface charge but reduced according to the free AuNPs that is supported in a reported study on gold loaded liposomes.<sup>27</sup>

**Table 1.** Size distribution and zeta potential of AuNPs, liposome, phytosome and AuNP-phytosomes. The data were presented by mean  $\pm$  SD<sup>a</sup> and n=3.

	Particle size (nm)	PDI	Zeta Potential (mV)
<b>AuNP</b>	8 $\pm$ 2	0.143 $\pm$ 0.009	-42 $\pm$ 7
<b>Liposome</b>	93 $\pm$ 6	0.093 $\pm$ 0.01	-31 $\pm$ 6
<b>Phytosome</b>	73 $\pm$ 6	0.118 $\pm$ 0.016	-18 $\pm$ 7
<b>AuNP-phytosome</b>	80 $\pm$ 5	0.264 $\pm$ 0.014	-22 $\pm$ 8

<sup>a</sup> $\pm$  SD values obtained from free-independent measurements of freshly prepared samples.

A short term size-dependent stability test (Fig 1 A) was carried out for 20 days using the vesicle formulations by keeping them at 4 °C. During 20 days, a dramatic change didn't observe at plain liposomes and phytosomes as well. On the other hand, the size of AuNP-phytosomes increased from 80 to 100 nm. It can be attributed to fusion of small sized vesicles or aggregation.<sup>7</sup> In the zeta potential-dependent stability, unlike other formulations, no significant change in the surface charge was observed only with AuNP-phytosomes. The zeta potential of plain liposomes and phytosomes was generally variable during 20 days (data not shown). It is well-known that if the phytosomes are kept in the state of suspension in a water environment for a long-term, the system would be destroyed due to the physical and chemical instability (PC hydrolysis from ester bonds, PC oxidation, Calendula extract leakage of vesicle bilayers) as well as the contamination (bacterial growth).<sup>28</sup> Therefore, it can be claimed that AuNPs may have an influence on extract compounds to keep them in more stable structure.

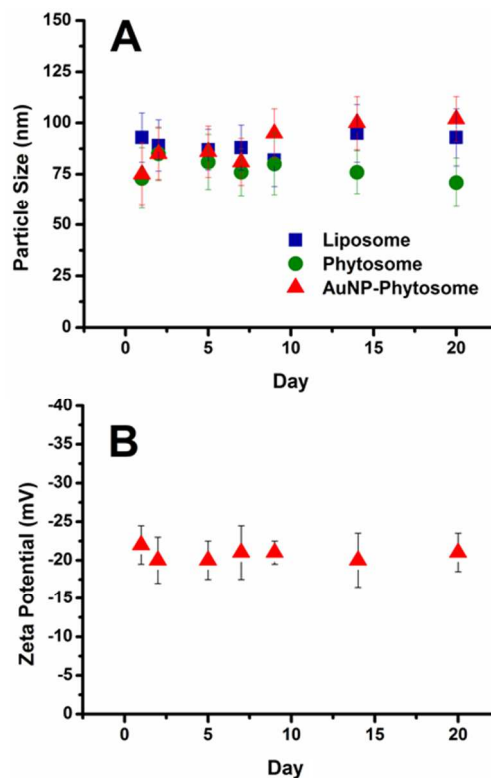


**Figure 1.** Short term size-dependent stability of prepared vesicles (A) and zeta potential-dependent stability of AuNP-phytosomes (B), (Error bars show the S.D of 3-4 trials).

Fig 2 represents the AFM images of the liposomes, prepared by using spin-coating method. We compared morphologies of three vesicle films prepared by spin casting processes. The bubble-like shape of the phytosome (Fig 2B) and AuNP-phytosome (Fig 2C) vesicles can be seen clearly from the height images of AFM. In addition, the nm scaled bars proves the particle size data that was measured with dynamic light scattering except plain liposomes.

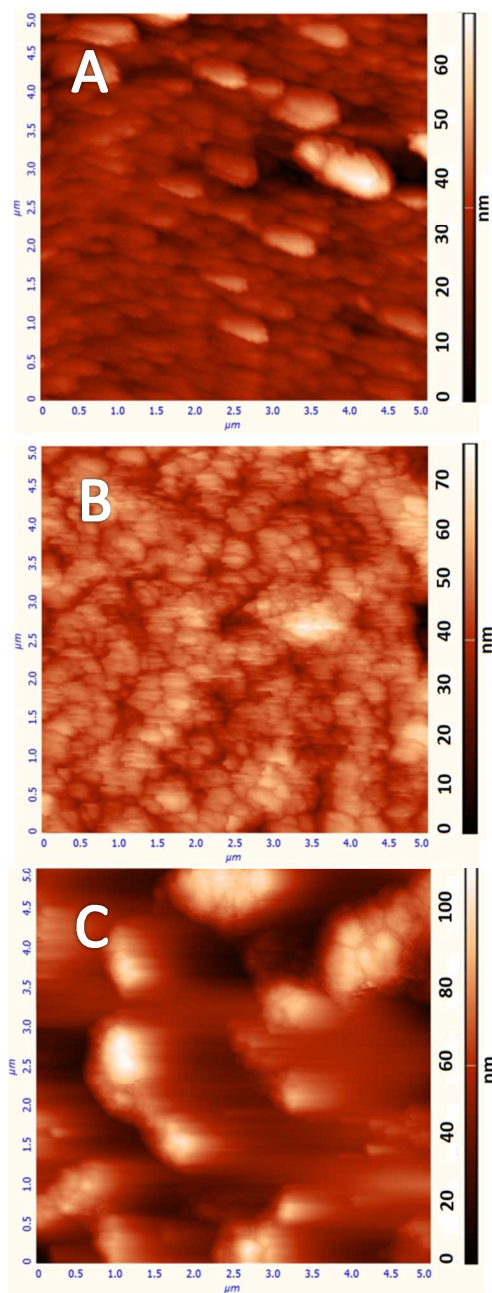


**Figure 2.** AFM height images (2.5x2.5) of plain liposomes (A), phytosomes (B) and AuNP-phytosomes (C).

### 3.2 Encapsulation efficiency of phytosomes and AuNP-phytosomes

To calculate the encapsulation efficiency (EE), different methods such as spectrophotometric and fluorimetric with a model fluorophore dye were used in the literature.<sup>29</sup> Upon the spectrophotometric ways used in total phenolic and flavonoid content experiments, EE of Calendula extract was obtained by UPLC according to the major compounds of phenolics (chlorogenic acid) and flavonoids (quercetin).<sup>30</sup> Prior to give the samples to UPLC column, standard curves for both chlorogenic acid (CA) and quercetin were constituted and the linear equations of the curves are found as  $y = 77.57x - 244.61$ , ( $R^2 = 0.999$ ) for CA with a linearity between 25 – 1000 ppb and  $y = 404.99x - 2889.1$ , ( $R^2 = 0.999$ ) for quercetin with a

linearity between 10 – 500 ppb. As a result, EE of phytosomes was calculated as 49% for CA and 77% for quercetin. In the case of AuNP-phytosomes, EE is 62% for CA and 86% for quercetin. It can be seen that quercetin based EE gave higher results in comparison with CA ( $p < 0.05$ ). It could be explained by the fact that a unit of phytosome is usually flavonoid molecule linked with at least one PC molecule.<sup>31</sup> AuNP-phytosome formulation illustrates a better EE (%) than phytosomes in considering with both major compounds. As can be seen from the zeta potential stability and EE data, there might be a supportive interaction between AuNPs and the plant extract that caused more stable preparations. In the other studies where AuNP and other encapsulated materials are used<sup>32</sup>, there is no similar result in the literature.

### 3.3 Cell culture studies

After characterization, cytotoxicity, cell-based antioxidant activity, *in vitro* wound healing with scratch assay and cell imaging studies were investigated for the AuNP-phytosomes. In these studies, AuNPs, Calendula extract, plain liposome and phytosomes without AuNP were also tested to compare with AuNP-phytosomes as the control.

**Cytotoxicity of AuNP-phytosomes.** The cytotoxic activity of AuNP-phytosomes was evaluated at different concentrations of plain liposomes and phytosomes as well. The initial concentrations of AuNPs ( $50 \mu\text{g mL}^{-1}$ ) and *C. officinalis* extract ( $500 \mu\text{g mL}^{-1}$ ) were treated at varying concentrations in order to compare with vesicular formulations. Fig 3 exhibits the cell viability after treatment with samples.

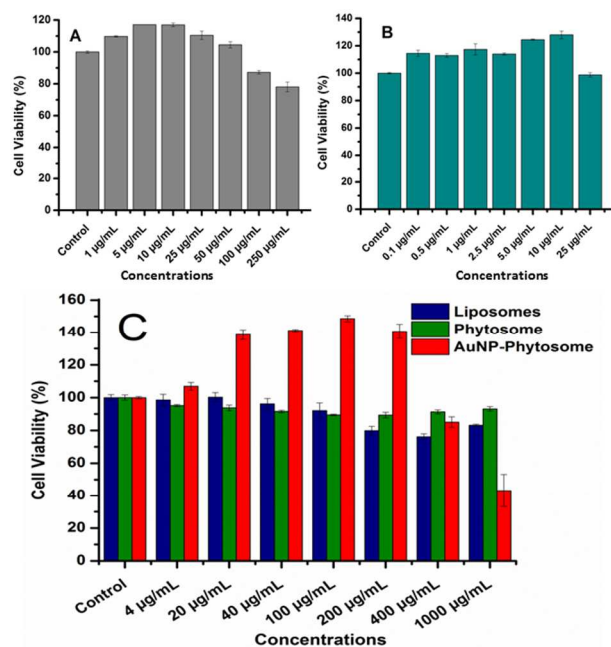


**Figure 3.** *In vitro* cytotoxicity assays for the Calendula extract (A), AuNP (B) and vesicle formulations (C) using Vero cells after 2 h incubation in MEM medium with 10% FCS and 5.0% CO<sub>2</sub> humidified air. Error bars mean  $\pm$ S.D, (n=3).

Calendula extract in  $500 \mu\text{g mL}^{-1}$  stock solution equals to 12 ppm CA showed no considerable decrease following the treatment until  $50 \mu\text{g mL}^{-1}$  (1.2 ppm CA). The increase of extract amount from 50 to  $250 \mu\text{g mL}^{-1}$  led to 20% toxicity

against control that contains no extract. Additionally, AuNPs dissolved in PBS ( $50 \mu\text{g mL}^{-1}$ ) were added to cells and any toxic effect was not seemed in compared to the control (Fig 3B). This data is in agreement with the other studies concerning the AuNPs as non-toxic nanomaterials.<sup>15b</sup> Moreover, Fig 3B illustrates that AuNPs increased the cell viability in compared to the control group as well. In the case of vesicular formulations, dilutions were calculated according to total lipid amounts (PC and Chol) where stock solution is  $2.0 \text{ mg mL}^{-1}$ , because of different %EE and the presence of AuNP in the AuNP-phytosome formulation. According to data, the acceptable non-toxic concentration of the plain liposomes is up to  $100 \mu\text{g mL}^{-1}$ . As for phytosomes (where stock solution has  $6.0 \text{ ppm CA}$ ), all concentrations up to the  $1000 \mu\text{g mL}^{-1}$  were appeared to be non-toxic to the Vero cells. As the final step, AuNP-phytosomes did not exhibit any toxic effect up to  $400 \mu\text{g mL}^{-1}$  (that contains  $1.6 \text{ ppm CA}$  and  $10 \mu\text{g mL}^{-1}$  AuNP). In contrast,  $1000 \mu\text{g mL}^{-1}$  AuNP-phytosomes ( $4.0 \text{ ppm}$  and  $25 \mu\text{g mL}^{-1}$  AuNP) decreased the cell viability to 43%. It is a fact that in order to assess the further investigations including antioxidant activity and scratch assay, a non-toxic mean concentrations have to be selected. These doses are as followed for the samples;  $5.0 \mu\text{g mL}^{-1}$  ( $0.12 \text{ ppm CA}$ ) for Calendula extract,  $0.5 \mu\text{g mL}^{-1}$  for AuNP and  $20 \mu\text{g mL}^{-1}$  lipid concentrations (for phytosome  $0.06 \text{ ppm CA}$  content and for AuNP-phytosome  $0.08 \text{ ppm CA}$  content and  $0.5 \mu\text{g mL}^{-1}$  AuNP occurs) for the rest of the formulations. It can be claimed that the difference between effect of phytosome and AuNP-phytosome on the cell viability could be mainly occurred due to the EE of CA in the vesicles. Moreover, the cell-material interactions in which AuNP-phytosome stimulates the antioxidant features could be also effective on this parameter.

#### Cell-based antioxidant capacity.

The reactive oxygen species (ROS) which have unpaired electrons generated during oxidative metabolism, such as ( $\text{O}_2^-$ ) ions,  $\cdot\text{OH}$  radicals or hydrogen peroxide ( $\text{H}_2\text{O}_2$ ) molecules are eliminated in biological systems. They may cause oxidative damage to biomacromolecules consist of DNA, proteins and lipids in cell. Hence, the ROS display significant roles in the regulation of apoptosis and cell proliferation mechanisms.<sup>33</sup> The antioxidant capacity of phytosomes and other samples including free AuNP and Calendula extract were estimated within  $\text{H}_2\text{O}_2$  damage of Vero cells after 24 h. Fig 4 exhibits the protective effect of pre-treated Vero cells with samples with the selected concentrations as mentioned in cytotoxicity part. According to Fig 4, plain liposomes and phytosomes were not shown any considerable protective effect after the addition of  $\text{H}_2\text{O}_2$  to the cells. Furthermore, free Calendula extract decreased the cell viability at the selected amount in compared to its vesicular formulation and un-treated Vero cells which has 48.8% of the viability ( $p < 0.01$ ). On the other hand, AuNPs that was  $0.5 \mu\text{g mL}^{-1}$  in growth medium and AuNP-phytosomes protected the cells as the ratio of 74% and 81%, respectively. These results were in an agreement with the cytotoxicity assay of samples because the enhanced activity of AuNPs and Calendula in the vesicular forms has been observed. It can be claimed that AuNP-phytosome formulation has higher antioxidative effect among other samples ( $p < 0.05$  for all samples except free AuNPs).

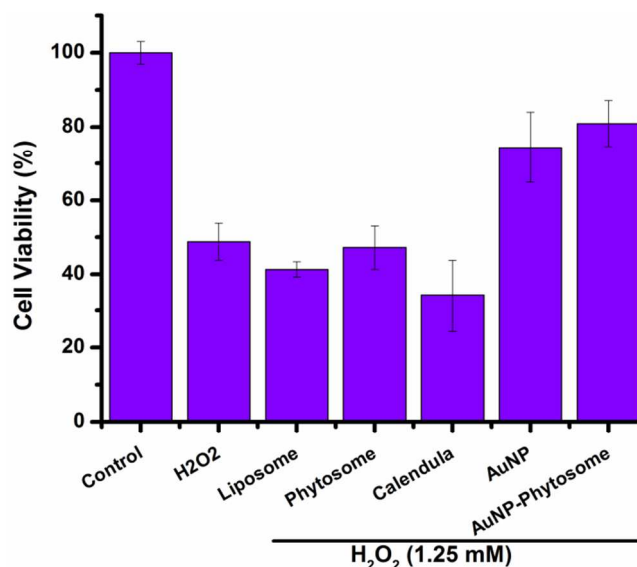


**Figure 4.** Influence of  $\text{H}_2\text{O}_2$  ( $1.25 \text{ mM}$ ) on the cell viability of Vero cells pre-treated with samples. Error bars mean  $\pm$ S.D, ( $n=3$ ).

**In vitro scratch assay for wound healing.** In order to measure the cell migration and wound healing on *in vitro* platforms, scratch assay have been an easy, low-cost and well-developed method by comparing this to *in vivo* investigations. The latter phase of wound healing is characterized by proliferation and migration of either keratinocytes or fibroblasts and a parallelism within scratch assay is observed.<sup>34</sup> The procedure of this method forms from a few basic steps including creation a scratch in cell monolayer, monitoring the cell behaviour at the beginning and fixed time intervals and comparing to the captured images to quantify the migrated cells.<sup>35</sup> Additionally, scratch assay were performed in many studies based on wound healing potential of bioactive compounds and bio-nanomaterials.<sup>22a</sup> To represent the wound healing potential of phytosomal samples besides free encapsulated materials (Calendula and AuNPs), NHDF cells were growth in multi-well plates and closure of the cells were analysed via Image J software at 4 and 8 h. As shown in Fig 5, all samples which were added to the growth medium have an influence upon artificial wounds for the NHDF cell monolayer except plain liposomes (23.5%) after 8 h treatment. In the previous antioxidant activity study, free Calendula extract have not generate a difference in compared to the control groups (27.42% for 8 h), ( $p < 0.05$ ). However, there is a slight change in cell proliferation for  $5.0 \mu\text{g mL}^{-1}$  Calendula extract and  $0.5 \mu\text{g mL}^{-1}$  AuNPs as 35.7% and 31.6%, respectively. Since vesicular formulations of Calendula and AuNPs have lower content according to their free forms, they accelerated the gap closure of cell monolayer about 42.2% for phytosomes and 58.7% for AuNP-phytosomes ( $p < 0.01$ ). In another studies, hexane and ethanolic extracts of Calendula flowers for 1.0 and  $10 \mu\text{g mL}^{-1}$  concentrations have showed an increase in 3T3 albino mouse fibroblasts.<sup>22b</sup> This data supports our findings as well.

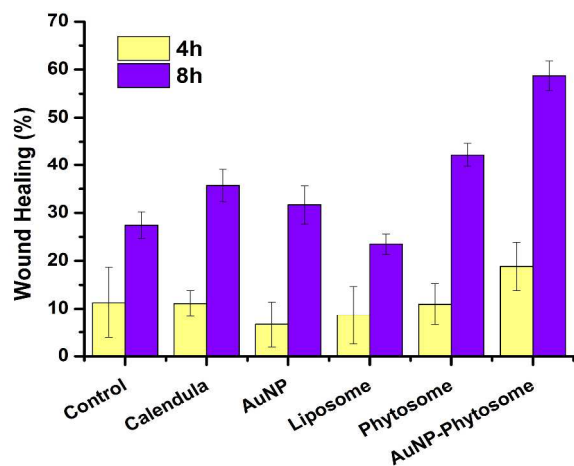


**Figure 5.** Wound healing effect of samples on NHDF cells at 4 and 8 h. Data are expressed as percent of gap closure in the wounded area compared to the control. Error bars mean  $\pm$ S.D (n=3).

**Cell imaging studies.** Efficient delivery of bioactive materials into the living cells is major biotechnological challenges. To understand and represent the effective delivery of vesicular formulations including liposomes, phytosomes and AuNP-phytosomes, aromatic group labelled Texas-Red DHPE lipid were introduced as part of the fluorescence cell imaging study. Among other aromatic group labelled lipids, Texas-red labelled one is more attributed to utilize in cell imaging experiments.<sup>36</sup> Therefore, Texas-Red labelled DHPE lipid was added to the formulations as 0.05 mg ratio (given in material and methods section) to visualize the penetration of lipid vesicles into the Vero cells. Fig 6 (A-C) shows the cell images obtained by merging of both Texas-Red labelled and DAPI stained cells for the following three formulations; plain liposomes, phytosomes and AuNP-phytosomes. For the imaging studies, red filter for Texas-Red labelled vesicles and blue filter for DAPI staining were used. Besides, green filter were utilized for the AuNP loaded phytosomes which exhibits fluorescence properties (Fig 6D). In the literature, the fluorescence properties of AuNPs were studied by He et al. and Huang et al. and they reported the use of anti-epidermal growth factor receptor conjugated AuNPs in both bright-field and fluorescence microscopy upon HeLa and HaCaT cell lines (human keratinocytes).<sup>37</sup> The cell images of Texas-Red labelled vesicles are in line with other results that proves the biological effect of AuNPs in phytosomes. By comparing plain liposome, cell penetration of extract incorporating vesicles and especially AuNP loaded phytosomes was observed more efficiently and particularly around the nucleus of the cells.

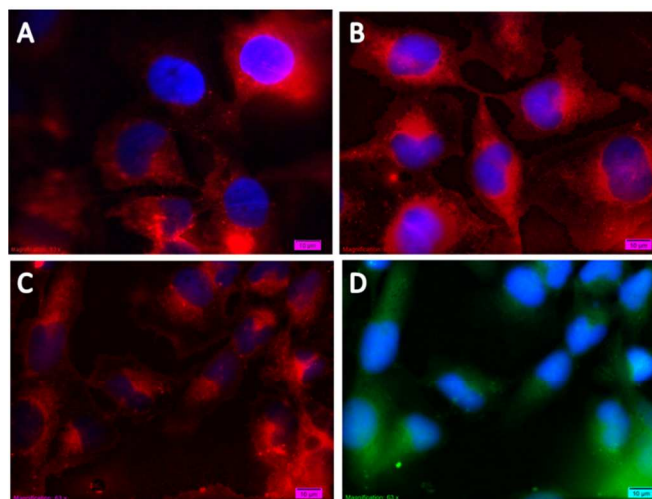


**Figure 6.** Fluorescence microscope images of the Texas-Red labelled plain liposomes (A), phytosomes (B) and AuNP-phytosomes (C and D) with Vero cells. The images were created by overlapping of the images of cells treated with Texas-Red labelled vesicles and images of cells stained with DAPI. Scale bars of each image are 10  $\mu$ m.

## Conclusion

We showed here, the first double encapsulation of a herbal extract and nanoparticles by using Calendula and AuNPs as ‘AuNP-phytosomes’ in a comprehensive comparing among free AuNP and Calendula extract for cell culture studies and plain liposomes and phytosomes for all through the study. The resulting AuNP-phytosomes exhibited remarkably high stability among the other formulations used for comparison and also have higher EE according to its phytosome form. At the same time, the cell culture studies were accomplished successfully with the AuNP-phytosome which has no toxic effect up to 400  $\mu$ g mL<sup>-1</sup> and higher antioxidant capacity as well as wound healing properties. In the next part of the work based on fluorescence imaging, it was shown that the formulated vesicles that were under 100 nm, could penetrate to the cells and accumulate around nucleus. Within this approach, the biological activity of AuNP and Calendula extract were enhanced and this formulation can create new ideas upon producing novel dermo-cosmetic and pharmaceutical preparations.

## Acknowledgements

This study was funded by Industrial thesis support program (SANTEZ) by Ministry of Science, Industry and Technology. And also this work was partially supported by Ege University Scientific Research Project (2013/FEN/024). Ege University Aliye Uster Foundation was also acknowledged for the research grants. Authors were grateful to WATERS Corp. for supplying UPLC system.

## Notes and references

<sup>a</sup> Ege University, Faculty of Science, Biochemistry Department, 35100-Bornova, Izmir, TURKEY.

<sup>b</sup> Ege University, Institute of Drug Abuse Toxicology & Pharmaceutical Sciences, 35100-Bornova, Izmir, TURKEY.

- <sup>c</sup> Izmir Katip Celebi University, Faculty of Engineering and Architecture, Material Science and Engineering Department, 35620-Cigli, Izmir, TURKEY.
- <sup>d</sup> Dicle University, Faculty of Science, Chemistry Department, 21280-Diyarbakir, TURKEY.
- <sup>e</sup> Ege University, School of Medicine, Department of Psychiatry, 35100-Bornova, Izmir, TURKEY.
- <sup>f</sup> Ege LS, Ege University, 35100-Bornova, Izmir, TURKEY
- 1 (a) Y. Malam, M. Loizidou and A. M. Seifalian, *Trends Pharmacol. Sci.*, 2009, **30**, 592–599; (b) R. R. Sawant and V. P. Torchilin, *Soft Matter*, 2010, **6**, 4026–4044; (c) M. L. Tan, P. F. Choong and C. R. Dass, *Peptides*, 2010, **31**, 184–193; (d) A. C. Oliveira, M. P. Ferraz, F. J. Monteiro and S. Simoes, *Acta Biomater.*, 2009, **5**, 2142–2151; (e) F. Xiong, Z. Mi and N. Gu, *Pharmazie*, 2011, **66**, 158–164; (f) K. Bourzac, *Nature*, 2012, **491**, S58–S60; (g) H. Lusic and M. W. Grinstaff, *Chem. Rev.*, 2013, **113**, 1641–1666.
  - 2 C. Manach, A. Scalbert, C. Morand, C. Rémésy and L. Jiménez, *Am. J. Clin. Nutr.*, 2004, **79**, 727–747.
  - 3 (a) M. Fan, S. Xu, S. Xia and X. Zhang, *J. Agric. Food Chem.*, 2007, **55**, 3089–3095; (b) A. Karewicz, D. Bielska, B. Gzyl-Malcher, M. Kepczynski, R. Lach and Maria Nowakowski, *Colloid Surface B*, 2011, **88**, 231–239; (c) D. Yang, L. Gan, J. Shin, S. Kim, S. Hong, S. Park, J. Hee Lee and K. Lee, *J. Food Sci.*, 2013, **78**, 43–49; (d) P. Rijo, D. Matias, A. S. Fernandes, M. F. Simões, M. Nicolai and C. P. Reis, *Polymers*, 2014, **6**, 479–490; (e) M. Gibis, E. Vogta and J. Weiss, *Food Funct.*, 2012, **3**, 246–254; (f) H. Yu, J. Li, K. Shi and Q. Huang, *Food Funct.*, 2011, **2**, 373–380.
  - 4 E. Bombardelli, S. B. Curri, R. L. Della, N. P. Del, A. Tubaro and P. Gariboldi, *Fitoterapia*. 1989, **60**, 1–9.
  - 5 (a) E. Bombardelli, *Boll. Chim. Farm.*, 1991, **130**, 431–438; (b) D. Peer, J. M. Karp, S. Hong, O. C. Farokhzad, R. Margalit and R. Langer, *Nat. Nanotechnol.*, 2007, **2**, 751–760.
  - 6 (a) P. Kidd and K. Head, *Altern Med Rev.*, 2005, **10**, 193–203; (b) E. Bombardelli, M. Spelta, R. Loggia Della, S. Sosa and A. Tubaro, *Fitoterapia*, 1991, **62**, 115–22.
  - 7 Z. Hou, Y. Li, Y. Huang, C. Zhou, J. Lin, Y. Wang, F. Cui, S. Zhou, M. Jia, S. Ye and Q. Zhang, *Mol. Pharmaceutics*, 2013, **10**, 90–101.
  - 8 (a) A. Dahan, R. Duvdevani, I. Shapiro, A. Elmann, E. Finkelstein and A. Hoffman, *J. Controlled Release*, 2008, **126**, 1–9; (b) A. Federico, M. Trappoliere, C. Tuccillo, I. de Sio, A. Di Leva, C. Del Vecchio Blanco and C. Loquercio, *Gut*, 2006, **55**, 901–902; (c) Y. Lu, Y. Zhang, Z. Yang and X. Tang, *Int. J. Pharm.*, 2009, **366**, 160–169; (d) K. Maiti, K. Mukherjee, A. Gantait, B. P. Saha and P. K. Mukherjee, *Int. J. Pharm.*, 2007, **330**, 155–163; (e) Q. Peng, Z. R. Zhang, X. Sun, J. Zuo, D. Zhao and T. Gong, *Mol. Pharmaceutics*, 2010, **7**, 565–575; (f) D. Singh, M. S. Rawat, A. Semalty and M. Semalty, *Curr. Drug Delivery*, 2012, **9**, 305–314; (g) W. Wei, S. J. Shi, J. Liu, X. Sun, K. Ren, D. Zhao, X. N. Zhang, Z. R. Zhang and T. Gong, *J. Drug Targeting*, 2010, **18**, 557–566; (h) K. Xu, B. Liu, Y. Ma, J. Du, G. Li, H. Gao, Y. Zhang and Z. Ning, *Molecules*, 2009, **14**, 3486–3493; (i) X. Yanyu, S. Yunmei, C. Zhipeng and P. Qineng, *Int. J. Pharm.*, 2006, **307**, 77–82; (j) P. F. Yue, H. L. Yuan, X. Y. Li, M. Yang and W. F. Zhu, *Int. J. Pharm.*, 2010, **387**, 139–146; (k) Z. Zhang, Y. Huang, F. Gao, H. Bu, W. Gu and Y. Li, *Nanoscale*, 2011, **3**, 1780–1787.
  - 9 J. A. Duke, M. J. Bogenschutz-Godwin, J. Du Celliar, P. A. K. Duke. *Hand Book of Medicinal Herbs*, 2nd ed. CRC Press, Boca Raton, pp. 2002, 139–140.
  - 10 E. Jiménez-Medina, A. Garcia-Lora, L. Paco, I. Algarra, A. Collado and F. Garrido, *BMC Cancer*, 2006, **6**, 119–134.
  - 11 K. Zitterl-Eglseer, S. Sosa, J. Jurenitsch, M. Schubert-Zssilavec, R. Della Loggia, A. Tubaro, M. Bertoldi and C. Franz, *J. Ethnopharmacol.*, 1997, **57**, 139–144.
  - 12 V. Katalinic, M. Milos, T. Kulisic and M. Jukic, *Food Chem.*, 2006, **94**, 550–557.
  - 13 J. A. Wenninger and G. N. McEwen Jr. eds. *International cosmetic ingredient dictionary and handbook*, 7th ed. 1997, **1**, 186–187. Washington, DC: CTFA.
  - 14 P. Pommier, F. Gomez, M.P. Sunyach, A. D’Hombres, C. Carrie and X. Montbarbon. *J. Clin. Oncol.*, 2004, **22**, 1447–1453.
  - 15 (a) J. B. Delehanty, K. Boeneman, C. E. Bradburne, K. Robertson, J. E. Bongard and I. L. Medintz, *Ther. Deliv.*, 2010, **1**, 411–433; (b) D. A. Giljohann, D. S. Seferos, W. L. Daniel, M. D. Massich, P. C. Patel and C. A. Mirkin, *Angew. Chem. Int. Ed.*, 2010, **49**, 3280–3294; (c) R. A. Petros, and J. M. DeSimone. *Nat. Rev. Drug Discovery*, 2010, **9**, 615–627; (d) J. Shi, A. R. Votruba, O. C. Farokhzad, and R. Langer, *Nano Lett.*, 2010, **10**, 3223–3230; (e) P. M. Tiwari, K. Vig, V. A. Dennis and S. R. Singh, *Nanomaterials*, 2011, **1**, 31–63.
  - 16 W. T. Al-jamal and K. Kostarelos, *Acc. Chem. Res.*, 2011, **44**, 1094–1104.
  - 17 G. Wu, A. Mikhailovsky, H. A. Khant, C. Fu, W. Chiu and J. A. Zasadzinski, *J. Am. Chem. Soc.*, 2008, **130**, 8175–8177.
  - 18 R. Michel, T. Plostica, L. Abezgaus, D. Danino and M. Gradzielski, *Soft Matter*, 2013, **9**, 4167–4177.
  - 19 M. Gonzalez and V. Gonzalez, *Anal. Methods*, 2010, **2**, 1842–1866.
  - 20 D. Ag, R. Bongartz, L. Eral Dogan, M. Selecki, J.-G. Walter, D. Odaci Demirkol, F. Stahl, S. Ozcelik, S. Timur and T. Scheper, *Colloid Surface B*, 2014, **114**, 96–103.
  - 21 (a) H. Li, Z. Deng, R. Liu, S. Loewen and R. Tsao, *Food Chem.*, 2013, **136**, 878–888; (b) W. Zeng, W-C. Zhang, W-H. Zhang, Q. He and B. Shi. *Food Chem. Toxicol.*, 2013, **58**, 311–317.
  - 22 (a) J. Leu, S. Chen, H. Chen, W. Wu, C. Hung, Y. Yao, C. Tu and Y. Liang, *Nanomed: Nanotechnol.*, 2012, **8**, 767–775; (b) M. Fronza, B. Heinzmann, M. Hamburger, S. Lauferd and I. Merfort, *J. Ethnopharmacol.*, 2009, **126**, 463–467.
  - 23 J. Sabin, G. Prieto and F. Sarmiento, *Soft Matter*, 2012, **8**, 3212–3222.
  - 24 N. J. Alves, W. Cusick, J. F. Stefanick, J. D. Ashley, M. W. Handlogten and B. Bilgicer, *Analyst*, 2013, **138**, 4746–4751.
  - 25 G. Qin, S. Geng, L. Wang, Y. Dai, B. Yang and J-Y. Wang. *Soft Matter*, 2013, **9**, 5649–5656.
  - 26 G. M. M. El Maghraby, A.C. Williams and B.W. Barry, *Int. J. Pharm.*, 2004, **276**, 143–161.
  - 27 M. M. Mady, M. M. Fathy, T. Youssef and W. M. Khalil, *Phys. Medica*, 2012, **28**, 288–295.
  - 28 W. Abdelwahed, G. Degobert, S. Stainmesse and H. Fessi. *Adv. Drug Delivery Rev.*, 2006, **58**, 1688–1713.
  - 29 K. Sou, *Chem. Phys. Lipids*, 2011, **164**, 211–215.
  - 30 K. A. Khalid and J. A. Teixeira da Silva, *Medicinal Aromatic Plant Sci. Biotech.*, 2011, **6**, 12–27.

- 31 N. Jain, B. P. Gupta, N. Thakur, R. Jain, J. Banweer, D. K. Jain and S. Jain, *Int. J. Pharm. Sci. Drug Res.*, 2010, **2**, 224–228.
- 32 X. An, F. Zhang, Y. Zhu and W. Shen, *Chem. Commun.*, 2010, **46**, 7202–7204.
- 33 J. Bernatoniene, R. Masteikova, J. Davalgienė, R. Peciura, R. Gauryliene, R. Bernatoniene, D. Majiene, R. Lazauskas, G. Civinskiene, S. Velziene, J. Muselik and Z. Chalupova, *J. Med. Plants Res.*, 2011, **5**, 868–877.
- 34 (a) G. C. Gurtner, S. Werner, Y. Barrandon and M. T. Longaker, *Nature*, 2008, **453**, 314–321; (b) P. Martin, *Science*, 1997, **276**, 75–81.
- 35 C. C. Liang, A. Y. Park and J. L. Guan, *Nat Protoc.*, 2007, **2**, 329–333.
- 36 A. Csisza'r, N. Hersch, S. Dieluweit, R. Biehl, R. Merkel and B. Hoffmann, *Bioconjugate Chem.*, 2010, **21**, 537–543.
- 37 (a) H. He, C. Xie and J. Ren, *Anal. Chem.*, 2008, **80**, 5951–5957; (b) X. Huang, I. H. El-Sayed, W. Qian and M. A. El-Sayed, *J. Am. Chem. Soc.*, 2006, **128**, 2115–2120.